




# Studying fluctuating trajectories of optically confined passive tracers inside cells provides familiar active forces

URVASHI NAKUL,<sup>1,†</sup> SRESTHA ROY,<sup>1,†</sup> GOKUL NALUPURACKAL,<sup>1</sup>  
SNIGDHADEV CHAKRABORTY,<sup>1</sup> PRIYANKA SIWACH,<sup>1</sup> JAYESH  
GOSWAMI,<sup>1</sup> PRIVITA EDWINA,<sup>1,2</sup> SAUMENDRA KUMAR BAJPAI,<sup>2</sup>  
RAJESH SINGH,<sup>3,4,‡</sup> AND BASUDEV ROY<sup>1,5,‡</sup> 

<sup>1</sup>Department of Physics, Quantum Centre of Excellence for Diamond and Emergent Materials (QuCenDiEM), IIT Madras, Chennai 600036, India

<sup>2</sup>Department of Applied Mechanics, IIT Madras, Chennai 600036, India

<sup>3</sup>Department of Physics, IIT Madras, Chennai 600036, India

<sup>4</sup>rsingh@physics.iitm.ac.in

<sup>5</sup>basudev@iitm.ac.in

<sup>†</sup>Equal contribution

<sup>‡</sup>Equal corresponding authors

**Abstract:** In recent years, there has been a growing interest in studying the trajectories of microparticles inside living cells. Among other things, such studies are useful in understanding the spatio-temporal properties of a cell. In this work, we study the stochastic trajectories of a passive microparticle inside a cell using experiments and theory. Our theory is based on modeling the microparticle inside a cell as an active particle in a viscoelastic medium. The activity is included in our model from an additional stochastic term with non-zero persistence in the Langevin equation describing the dynamics of the microparticle. Using this model, we are able to predict the power spectral density (PSD) measured in the experiment and compute active forces. This caters to the situation where a tracer particle is optically confined and then yields a PSD for positional fluctuations. The low frequency part of the PSD yields information about the active forces that the particle feels. The fit to the model extracts such active force. Thus, we can conclude that trapping the particle does not affect the values of the forces extracted from the active fits if accounted for appropriately by proper theoretical models. In addition, the fit also provides system properties and optical tweezers trap stiffness.

© 2023 Optica Publishing Group under the terms of the [Optica Open Access Publishing Agreement](#)

## 1. Introduction

Colloidal particles are widely used in various fields [1–7], including biophysics, due to their ability to mimic biological systems [8–11]. In the field of biology, colloidal particles are used to study the nonequilibrium dynamics in living cells [9,12,13]. One of the most important properties of colloidal particles is their fluctuation behavior inside a living cell. The study of colloidal particle fluctuations can provide valuable information about the physical and chemical properties of the cell.

Several studies have been conducted to investigate the fluctuations of colloidal particles inside living cells [12–19]. In one such study, researchers used the fluctuation-dissipation theorem to analyze the Brownian motion of colloidal particles inside a living cell. The results of the study showed that the fluctuations of colloidal particles inside the cell were significantly different from the fluctuations of particles in a homogeneous fluid [12,20]. This difference was attributed to the presence of the cell membrane, cytoskeleton, and other intracellular components. Viscoelasticity

measurements reveal that the cell cytoplasm is a complex, heterogeneous, poro-viscoelastic environment [21–25].

Another study used particle-tracking microrheology to investigate the mechanical properties of living cells. The study focused on the fluctuations of colloidal particles inside the cell and found that the fluctuations were influenced by the cell's cytoskeleton [26–28]. The researchers concluded that the cytoskeleton played a crucial role in determining the mechanical properties of the cell. Further the cell is an active system and the active processes influence the fluctuation dynamics of a colloidal particle suspended in the cell's cytoplasm. Methods developed in [23,29] make use of the generalised Maxwell's model (Jeffery's model) of viscoelasticity to model the Brownian fluctuations of optically trapped probes inside a viscoelastic medium. This model perfectly explains the experimental behaviour of tracer particles inside a cell in the frequency range greater than 100 Hz where passive thermal fluctuations are larger than active forces. However experimental signatures considerably deviate from the predictions of this model at frequencies lower than 10-12 Hz where active forces are presumed to be dominant. Existing techniques resort to active rheology to distinguish non equilibrium active dynamics from passive thermal behaviour [13,20]. A recently developed method utilizes passive fluctuation time series to understand active mechanics [19]. We attempt to define a model where the effective behaviour of an optically trapped tracer particle under the combined action of thermal as well as active forces inside a cell can be explained.

The motion of a passive particle inside a harmonic potential is given by the Ornstein-Uhlenbeck process. However, the Ornstein-Uhlenbeck process assumes that the particle is in thermal equilibrium with its surroundings, which may not be the case for microparticles inside cells. To account for this, researchers have developed an extension of the Ornstein-Uhlenbeck process known as the active Ornstein-Uhlenbeck particle [30,31]. The active Ornstein-Uhlenbeck particle takes into account the fact that microparticles inside cells are subject to active forces, such as those generated by molecular motors. These forces can cause the particle to move in a non-random manner, which cannot be described by the standard Ornstein-Uhlenbeck process. By incorporating active forces, this model can capture the non-random motion of particles and provide insights into the underlying biological processes [32,33]. We use the active Ornstein-Uhlenbeck theory [30,31] in combination with a previously utilized Jeffery's model or the generalized Maxwell's model [29,34–36] to make a fit to the power spectral density (PSD) of the fluctuations of a passive tracer inside the cell cytoplasm. The high frequency behaviour gives mechanical properties of the cytoplasm while the low frequency behaviour reveals the active nature of the fluctuations. The cross over from active to passive fluctuations appears to happen between 10 to 100 Hz of PSD. In addition, the high frequency part of the PSD provides the optical tweezers parameters like local trap stiffness inside the cell which are notoriously difficult to obtain otherwise.

## 2. Experimental system

### 2.1. Optical tweezers setup

The experiments are carried out with an inverted microscope configuration integrated with optical tweezers setup built with Optical Tweezers kit, OTKB/M from Thorlabs. The schematic of the setup is shown in Fig. 1(a). 1064nm beam from the laser source is passed through a polarising beam splitter. This polarised laser beam reflects off a dichroic mirror inclined at 45° towards the objective lens. We use an oil immersion, high numerical aperture (100X, 1.3NA, Nikon) objective which besides tightly focusing the beam at the sample chamber, also serves for high magnification imaging. At the sample plane, the highly focused IR beam can trap micron sized particles. The forward scattered light along with unscattered fraction of the beam passes onto the condenser. The outgoing light is reflected by another dichroic and passed through another polarising beam splitter. A half wave plate is used to compensate for the phase changes due to

the optical components. This mixture of forward scattered and unscattered polarised light from the polarising beam splitter is detected by the Quadrant Photodiode (QPD). QPD is connected to a Data Acquisition system (NI, USA) via a monitor. The DAQ is connected to a computer and all measurements are acquired and recorded using a Labview program.

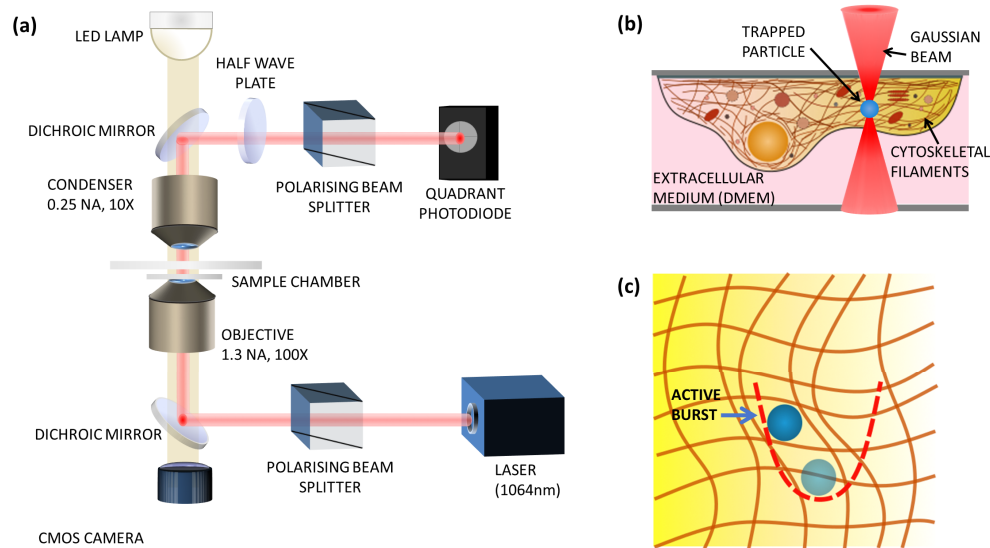


**Fig. 1.** (a) The schematic diagram of the experimental optical Tweezers setup. (b) shows an enlarged depiction of the sample chamber where the cell is attached to the upper surface of the sample chamber. Inside the cell, the cytoplasm is a complex environment having a nuclear region, cytoskeletal mesh, inhomogeneous viscoelastic cytosolic fluid with various organelles and proteins suspended in it. A particle phagocytosed by the cell is trapped at the focus of a laser beam. (c) schematically shows the theoretical model, a particle is caged within a mesh surrounded by a viscoelastic continuum (yellow shaded region). See text for details.

## 2.2. Preparation of living cells and getting a microparticle inside them

This experiment is performed on breast cancer cells (MCF-7). Cells are initially maintained in Dulbecco's modified Eagle medium (DMEM) at 37 C with 5% CO<sub>2</sub> in an incubator. Before seeding the cells, the glass coverslips are cleaned with detergent and then by acid wash using 1M HCl. The cleaned coverslips are then coated with a thin layer of 0.5% (by weight) aqueous solution of bacteriological gelatin (Thermo Fischer Scientific) to allow the cells to adhere to the surface. To do this we place a drop of the gelatin solution at the centre of the coverslip, allow it to spread, and then incubate it at 37 C for 1 hour. Cells are pelleted using a centrifuge and then resuspended in DMEM with an approximate concentration  $\sim 10^3$  cells/ml. A drop of the cell suspension is placed at the centre of the gelatin coated coverslip and placed in the incubator and wait for the cells to attach. Once the cells attach to the glass surface, the coverslip is washed with phosphate buffered saline solution. Sufficient amount of fresh media mixed with a concentrated suspension of 1  $\mu$ m sized polystyrene microparticles are added to the petridish containing the seeded coverslip. It is incubated at 37 C with 5% CO<sub>2</sub> for 24 hours till the cells attain about 70% confluency and have ingested the microparticle via phagocytosis.

### 2.3. Experiment

Cells maintained in DMEM media are placed in the sample chamber. Sample chamber is constructed by placing another glass coverlip on the coverslip containing MCF-7 cells. It is then placed between the condenser and objective on the sample stage. The sample chamber is placed in inverted position such that the cells are attached to the upper surface of the sample chamber (Fig. 1. (b)). 1064nm laser is focussed on the sample chamber through the objective. The sample stage can be moved in X,Y and Z direction. Particles inside the living cell are brought at the focus of the laser to trap it. Laser power is maintained at about 50mW at the sample plane, which has been focused with an objective of numerical aperture 1.3, such that the spot diameter is diffraction limited at about 1  $\mu\text{m}$ . We limit the laser exposure to not more than 1 minute at each location inside the cell, thereby reducing chances of heating. It is known in the community that laser powers in excess of 100 mW start to heat up the cells significantly [37]. Forward scattered light from the sample plane is collected by the condenser and split into two orthogonal components by the polarising beam splitter. Forward scattered intensity of the transmitted component of light is detected by the quadrant photodiode (QPD). A half wave plate is placed before the polarising beam splitter to ensure that light falling on QPD has same polarization as the incoming beam. Time series and its Fourier Transforms (Power Spectral Densities or PSD) for translational fluctuations are recorded with the Labview program from the signal from the QPD at a sampling rate of 40kHz.

## 3. Results and discussion

### 3.1. Theory

#### 3.1.1. Model

One of the challenges in studying colloidal particles in living cells is the viscoelastic nature of the intracellular environment. The viscoelasticity of the medium can affect the behavior of colloidal particles inside the cell and must be taken into account when analyzing their fluctuations [38,39]. Another crucial feature of the intracellular environment is the activity which affects the fluctuation and response of a microparticle embedded into it. Techniques such as particle-tracking microrheology have been developed to measure the mechanical properties of the cell and provide insights into the behavior of microparticles in such active environment [18,40–44]. We model a fluctuating trapped microparticle inside a cell as an active particle in a viscoelastic medium [13,30,31,45] enmeshed within a cytoskeletal cage (Fig. 1(c)). The equation of motion of the optically trapped microparticle located at a point  $x(t)$  at time  $t$  is given in terms of the following Langevin equation:

$$\int \gamma(t-t') \dot{x}(t') dt' = -\kappa x(t) + f_a(t) + \zeta(t), \quad (1)$$

where  $\zeta$  is a stochastic thermal force, which is a Gaussian colored noise with correlations  $C_\zeta(t) \equiv \langle \zeta(t)\zeta(0) \rangle = 2k_B T \Re[\gamma(t)]$ , as given by fluctuation dissipation theorem [46] and  $f_a$  is the active force, described below (Eq. (4) and (5)), and  $\kappa$  is the stiffness of the optical trap which depends on the intracellular environment. Here  $\Re[\dots]$  denotes real part of a complex number,  $k_B$  is Boltzmann constant and  $T$  is the bath temperature and  $\gamma$  is the frequency-dependent friction. The friction is obtained in terms of the viscosity  $\mu$  in an incompressible, low Reynolds number viscoelastic fluid obtained from Stokes-Oldroyd-B model. The viscoelasticity of the intracellular environment is assumed to be the contribution of protein polymers suspended in a purely viscous solvent. The frequency dependent viscoelasticity  $\mu$  is given as [23,25,29],

$$\mu(\omega) = \mu_s + \frac{\mu_p}{-i\omega\lambda + 1}. \quad (2)$$

Here  $\omega$  is the frequency,  $\mu_s$  is the zero-frequency solvent viscosity,  $\mu_p$  is the zero-frequency polymer viscosity and  $\lambda$  is the polymer relaxation time scale. Thus, we have:

$$\gamma(\omega) = \gamma_0 \left[ 1 + \frac{\mu_p}{\mu_s(-i\omega\lambda + 1)} \right] \quad (3)$$

and  $\gamma_0 = 6\pi\mu_s a_0$ . Here,  $a_0$  is the radius of the spherical tracer particle. The dynamics of the active force  $f_a$  is given as:

$$\tau \dot{f}_a(t) = -f_a + f_0 \sqrt{2\tau} \xi. \quad (4)$$

Here  $\xi$  is a white noise, while  $\tau$  is the persistence time. The persistence time  $\tau$  in this model sets the exponential decay of the two-point correlations:

$$C_A(t) \equiv \langle f_a(t) f_a(0) \rangle = f_0^2 e^{-|t|/\tau} = \gamma_a^2 v_0^2 e^{-|t|/\tau}. \quad (5)$$

Thus, the active force  $f_a$  can be viewed as a fluctuating force acting on the microparticle from the intracellular medium exerting an active drag  $\gamma_a$  and  $v_0$  being the active velocity of the particle. The burst of active force acts in a way to restructure the local potential formed by the optical trap and the cytoskeletal cage, causing the particle to move to the minima (red parabola in Fig. 1(c)). Unlike the fluctuating force from the thermal bath, this force has some persistence with a decorrelation time  $\tau$ . Thus, the motor-driven active fluctuations of microparticles in the intracellular medium is modeled using the active force  $f_a$ . We note that such a method to model stochastic active force  $f_a$  as an additional noise with some persistence has been used before to study trajectories of a passive tracer inside a cell [9,20] and also in the context of the motion of active particles [30,31]. We now use the model described above to obtain an explicit expression of the PSD (power spectral density) from fluctuating trajectories of microparticles and compare it with experimental data.

### 3.1.2. Power spectral density (PSD)

The PSD of the dynamical system defined in Eq. (1) is:

$$\text{PSD}(\omega) = C_x(\omega) = \langle x(\omega) x^*(\omega) \rangle. \quad (6)$$

Here  $x(\omega)$  is the Fourier transform of  $x(t)$ , while  $x^*(\omega)$  is the complex conjugate of  $x(\omega)$ . The expression for  $x(\omega)$  follows from a expansion of Eq. (1) in Fourier series. Explicitly, it is given as

$$x(\omega) = \frac{f_a(\omega) + \zeta(\omega)}{-i\omega \gamma(\omega) + \kappa} \quad (7)$$

Using the above form of  $x(\omega)$ , the explicit expression of the PSD is obtained as:

$$\text{PSD}(\omega) = \beta^2 \frac{S_a \left( \frac{1 + \omega^2 \lambda^2}{1 + \omega^2 \tau^2} \right) + A \left( \omega^2 + \frac{p}{\lambda^2} \right)}{\left( \frac{q}{\lambda} - \omega^2 \right)^2 + \omega^2 \left( q + \frac{p}{\lambda} \right)^2} + y_0. \quad (8)$$

In the above, a constant  $y_0$  is added to the power spectra density to account for the system noise floor, while  $\beta$  is a calibration factor. The remaining factors are described below:

$$S_a = \frac{2f_a^2 \tau}{\gamma_0^2 \lambda^2 \beta^2}, \quad (9)$$

$$A = \frac{2k_B T}{\gamma_0 \beta^2}, \quad (10)$$

$$p = 1 + \frac{\mu_p}{\mu_s}, \quad (11)$$

$$q = \frac{\kappa}{\gamma_0}. \quad (12)$$

The factor  $A$  can be calculated from the room temperature and viscosity coefficient of water at room temperature, as we describe below. The above expression has been used to compare with experimentally measured PSD. We find very good agreements as shown in Fig. (2) and Fig. (3). In systems where active force  $f_a = 0$ , Eq. (8) takes the form of Eq. (13), given below, which is the form for PSD for pure Brownian motion in viscoelastic medium as obtained in [29]. We denote this as  $\text{PSD}^{\text{eqm}}$ , whose explicit form is:

$$\text{PSD}^{\text{eqm}}(\omega) = \beta^2 A \frac{\left(\omega^2 + \frac{p}{\lambda^2}\right)}{\left(\frac{q}{\lambda} - \omega^2\right)^2 + \omega^2 \left(q + \frac{p}{\lambda}\right)^2} + y_0. \quad (13)$$

We note that the above expression has been generalised to non-equilibrium settings in Eq. (8). From Eq. (13), the parameter  $\beta$  can be computed using:

$$\beta^2 = \frac{2k_B T}{\gamma_0 A}. \quad (14)$$

The coefficient  $A$  is the amplitude of the fit to the PSD using Eq. (13). The  $\beta$  coefficient provides the calibration factor which when multiplied with the the fluctuation amplitude in Volts, provides a value in nm.

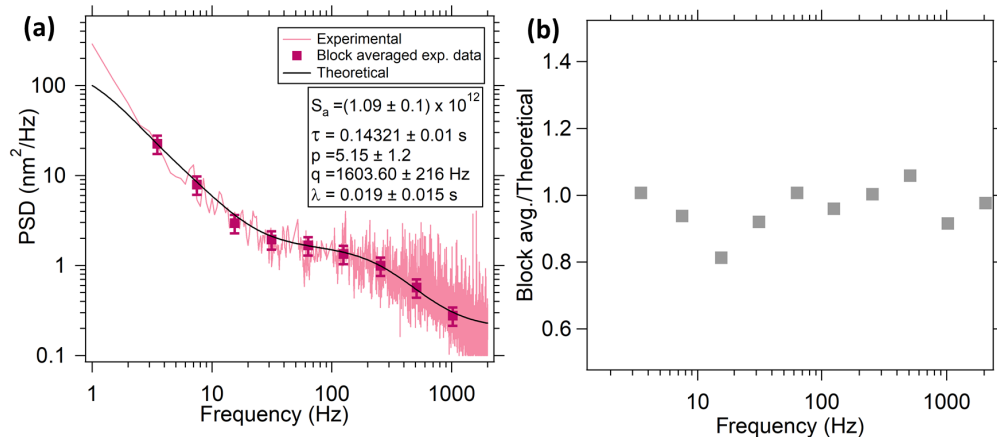


**Fig. 2.** (a) Experimentally obtained PSD for a particle inside the cell is shown in pink. The same PSD is block averaged logarithmically with a base of 2 and fitted to theoretical expression of Eq. (8). (b) shows that the ratios of the theoretical and experimentally obtained block averaged values which implies that the theory agrees well with the experimental values

### 3.2. Experimentally measured PSD

We then go on to fit the PSD function given in Eq. (8) to the experimentally obtained data. Since there are 6 parameters in the Eq. (8), we use a two step fitting routine. The passive thermal fluctuations dominate in higher frequency regions whereas active fluctuations come to prominence at lower frequency region. However the exact threshold where the crossover from



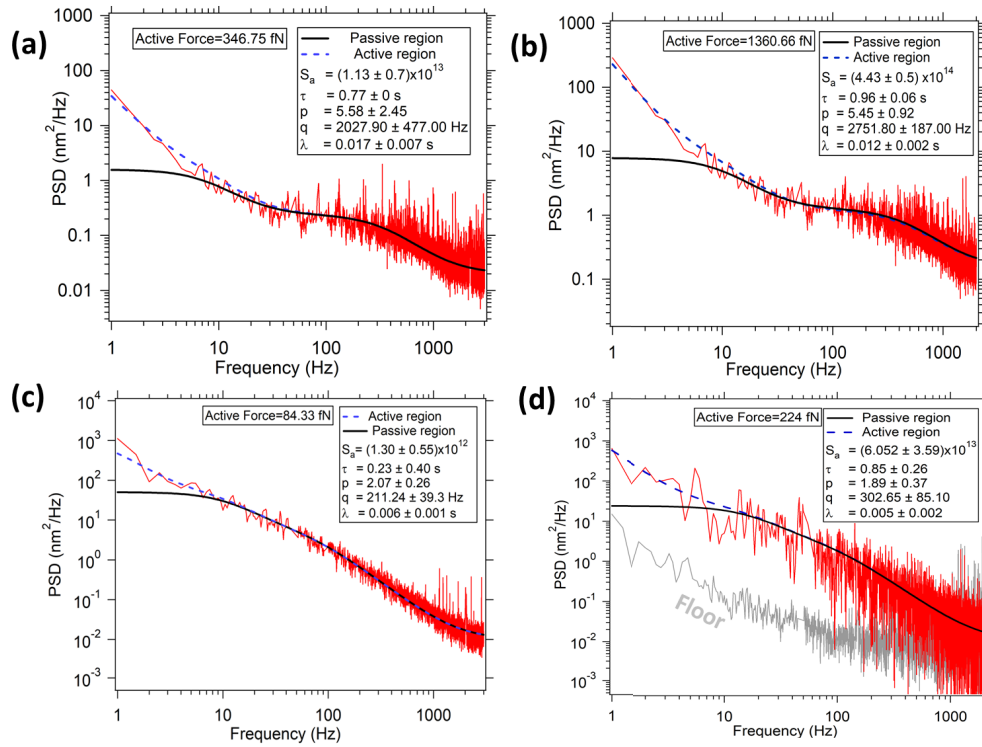


**Fig. 3.** (a)-(d) show PSDs measured for optically trapped particles inside different cells. Thermal passive fit is shown in black solid line considering  $f_a = 0$ . Blue dotted line shows the fit according to Eq. (8) considering both thermal and active fluctuations. The noise floor is shown in grey in (d) which accounts for spectra outside the cell devoid of activity

active to thermal dominance take place is imprecise and may differ from cell to cell depending on the external and internal condition of the cell. We find that almost always the activity of the cell goes to 0 in excess of 100 Hz [20]. Even amongst these, for many cells, the activity only extends till 10 Hz [47]. This is why, we mention that the transition happens between 10 Hz and 100 Hz. We choose a value of 20 Hz as the transition point. We therefore first fit the thermal spectrum to the PSD beyond 20 Hz by taking the active force  $f_a = 0$  which reduces the function to Eq. (13) 4 fitting parameters, viz.  $\beta^2$ ,  $p$ ,  $q$  and  $\lambda$  as has been reported earlier [23,25,29]. The parameter  $p$  is proportional to the ratio of polymer to solvent viscosity at 0 Hz and  $q$  gives an estimate of the local trap stiffness  $\kappa$  inside the cell. We then go on to lock the 4 passive parameters at these obtained values and then fit the PSD over the entire frequency range from 1 Hz to 3 kHz with Eq. (8) to ascertain all the parameters. The results are shown in Fig. 2(a), where we have block averaged the experimental data and fitted to the function. In order to estimate the quality of the fit with respect to the experimental data, we also take a ratio of the experimental data to the theoretical data and plot it in Fig. 2(b).

We also show a few typical fits in the Fig. 3. The black solid lines show the passive thermal region where  $f_a = 0$ . The deviation of the black solid lines from the experimental data shows the frequency domain where active fluctuations overcome thermal fluctuations. Blue dotted lines show the theoretical active region of the PSDs. It can be seen that the crossover from active to passive region do not occur at any definite frequency but varies from 5 Hz (Fig. 3(a)) to 10 Hz (Fig. 3(b)-(d)). We assume that the fit to the active region of the spectrum shall have the same mechanical parameters, namely  $p$  and  $\lambda$ , as the thermal region of the spectrum as its

the local property of the cytoplasm. While estimating the noise floor, the laser beam was made incident in the same fashion as while trapping but without the presence of the particle. This gives information about the laser noise and detector noise in the system.

We go on to compare the power law in the active region of the spectrum and compare with previously known facets. We find that the active region of the spectrum matches well with an exponent of  $-2$  (Fig. 4), as has been reported earlier [19,48]. Moreover, although we expect the PSD to form a plateau at low frequencies, it might actually be forming at an even lower frequency than has been detected in our measurements.

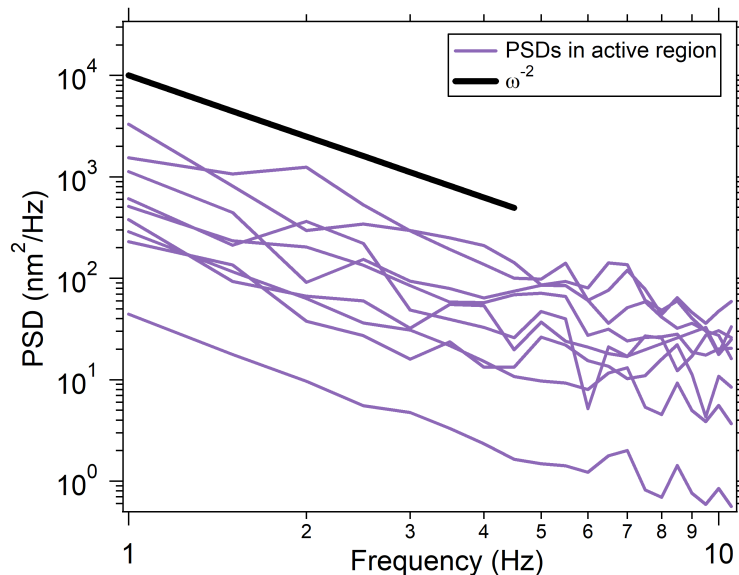


**Fig. 4.** The frequency regime from 1 Hz to 10 Hz shows dominance of active motion. The PSD follows a power law of  $-2$  with respect to frequency  $\omega$

We find a good fit to of the experimentally obtained PSD with that of the fit function. We then extract the parameters of the system from the fits and plot the distribution of the values in Fig. 5. We show measurements for 15 different cells, taken close to the periphery. The error bars have been propagated from the errors in the fit parameters. We find that the active forces range from 0.05 pN to about 1 pN, well compatible with the reports that it could either be molecular motor dynamics dominated like the myosin motors which apply 0 to 4 pN forces [20,49–52] or could be the activity of the mechano-enzymes [48]. The actual mechanism might require more investigation.

Thus, by using this technique, the active forces measured are well compatible to the previously obtained values even with the optical tweezers confining the probe particle. The time constants  $\tau$  provide information about the time scales over which the active forces act on the probe in the presence of the optical confinement. Our model automatically accounts for reduction in the fluctuations. We simultaneously find the cellular and optical tweezers parameters which can then be used to accurately apply controlled forces. We can envisage a situation where controlled forces can be applied to organelles. More sophisticated force application strategies could influence developmental biology problems like influencing fluid flows [53]. The exact implementation of the application of forces is however beyond the scope of the present manuscript.

Since the cells used in the experiment are alive, there is a lot of variability in the parameters ascertained. Even inside the same cell, the different regions may have different parameters. In fact, the same particle trapped in the same location of the cell might exhibit different power



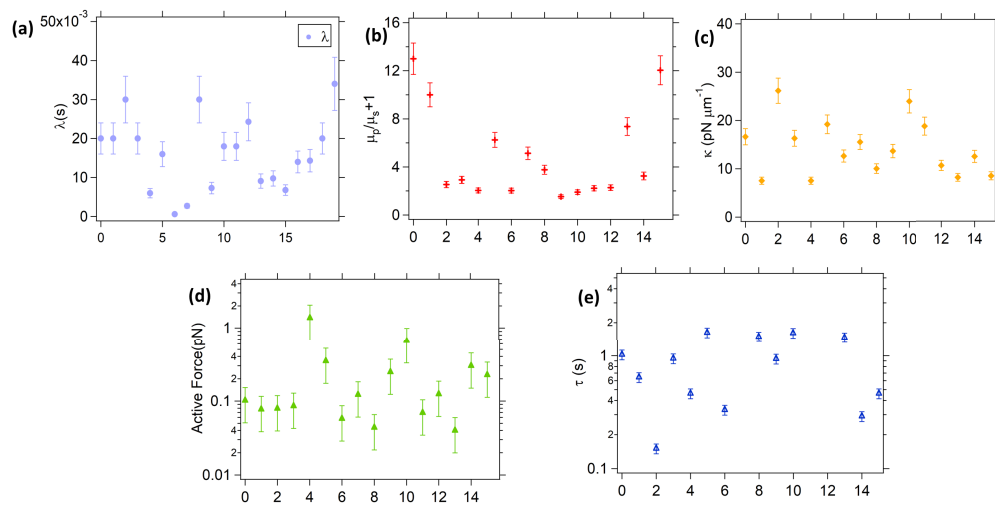


**Fig. 5.** Statistics of (a)-(c): Passive Parameters. (d)-(e): Active parameters measured for particles in 15 different cells, where the particles were close to the periphery of the cell.

spectrum due to the health of the cell, as has been reported in [25]. Merely tracking a particle trapped inside a cell at the same location, first immediately after placing it on microscope and then after a span of like 30 min changes the viscosity of the cytosol by almost a factor of 2. We report 15 events from 15 different cells, but highlight that these fit with the same expression for PSD. Variations due to the age, cell cycle, spatial region inside the cell and other factors are a matter for future research.

#### 4. Conclusion and perspectives

In conclusion, modelling a microparticle inside a cell as an active particle is a powerful tool for studying the dynamics of microparticles inside cells. Its ability to account for active forces provides a more accurate description of the motion of these particles and allows researchers to gain a deeper understanding of the biological processes at work [9]. We combine the high frequency fits to the passive thermal motion using microscopically derived generalised Maxwell's model with the Ornstein-Uhlenbeck model for activity to make a two-stage fit to the active and the passive processes. These studies have improved our understanding of the complex nature of living cells and can potentially lead to the development of new diagnostic tools for various diseases. There can be complementary strategies to cross-check the validity of the PSD technique utilized in this paper, such as, calculating the mean square displacement (MSD) and even invoking the rotational modes simultaneously to find correlations. However, both the exact derivation of such entities and their usage to study the fluctuations in the different modes is beyond the scope of the present manuscript. Indeed, these suggest exciting directions for further study.

**Funding.** Department of Biotechnology, Ministry of Science and Technology, India (IA/I/20/1/504900).

**Acknowledgements.** We thank the Indian Institute of Technology, Madras, India for their seed and initiation grants to BR and RS. This work was also supported in parts by the DBT/Wellcome Trust India Alliance Fellowship IA/I/20/1/504900 awarded to BR.

**Disclosures.** There are no conflicts of interest to declare.

**Data Availability.** Data underlying the results presented in this paper are not publicly available at this time but may be obtained from the authors upon reasonable request.

## References

- W. B. Russel, "Brownian motion of small particles suspended in liquids," *Annu. Rev. Fluid Mech.* **13**(1), 425–455 (1981).
- J. K. G. Dhont, *An Introduction to Dynamics of Colloids* (Elsevier, 1996).
- M. E. Cates and M. R. Evans, *Soft and Fragile Matter: Nonequilibrium Dynamics, Metastability and Flow* (Institute of Physics Publishing, 2000).
- M. Kleman and O. D. Laverntovich, *Soft Matter Physics: An Introduction* (Springer Science & Business Media, 2007).
- W. C. K. Poon, F. Renth, R. M. L. Evans, D. J. Fairhurst, M. E. Cates, and P. N. Pusey, "Colloid-polymer mixtures at triple coexistence: Kinetic maps from free-energy landscapes," *Phys. Rev. Lett.* **83**(6), 1239–1242 (1999).
- L. Berthier and G. Biroli, "Theoretical perspective on the glass transition and amorphous materials," *Rev. Mod. Phys.* **83**(2), 587–645 (2011).
- V. N. Manoharan, "Colloidal matter: Packing, geometry, and entropy," *Science* **349**(6251), 1253751 (2015).
- P. F. Luckham, "Manipulating forces between surfaces: applications in colloid science and biophysics," *Adv. Colloid Interface Sci.* **111**(1-2), 29–47 (2004).
- F. S. Gnesotto, F. Mura, J. Gladrow, and C. P. Broedersz, "Broken detailed balance and non-equilibrium dynamics in living systems: a review," *Rep. Prog. Phys.* **81**(6), 066601 (2018).
- E. Lauga, *The Fluid Dynamics of Cell Motility*, vol. 62 (Cambridge University Press, 2020).
- R. E. Goldstein, "Green algae as model organisms for biological fluid dynamics," *Annu. Rev. Fluid Mech.* **47**(1), 343–375 (2015).
- D. Mizuno, C. Tardin, C. F. Schmidt, and F. C. MacKintosh, "Nonequilibrium mechanics of active cytoskeletal networks," *Science* **315**(5810), 370–373 (2007).
- W. W. Ahmed, É. Fodor, and T. Betz, "Active cell mechanics: Measurement and theory," *Biochim. Biophys. Acta, Mol. Cell Res.* **1853**(11), 3083–3094 (2015).
- Y. Tseng, T. P. Kole, and D. Wirtz, "Micromechanical mapping of live cells by multiple-particle-tracking microrheology," *Biophys. J.* **83**(6), 3162–3176 (2002).
- É. Fodor, K. Kanazawa, H. Hayakawa, P. Visco, and F. Van Wijland, "Energetics of active fluctuations in living cells," *Phys. Rev. E* **90**(4), 042724 (2014).
- S. Yamada, D. Wirtz, and S. C. Kuo, "Mechanics of living cells measured by laser tracking microrheology," *Biophys. J.* **78**(4), 1736–1747 (2000).
- C. Wilhelm, "Out-of-equilibrium microrheology inside living cells," *Phys. Rev. Lett.* **101**(2), 028101 (2008).
- T. Toyota, D. A. Head, C. F. Schmidt, and D. Mizuno, "Non-gaussian athermal fluctuations in active gels," *Soft Matter* **7**(7), 3234–3239 (2011).
- T. M. Muenker, G. Knotz, M. Krüger, and T. Betz, "Onsager regression characterizes living systems in passive measurements," *bioRxiv*, bioRxiv:2022.05.15.491928 (2022).
- W. W. Ahmed, É. Fodor, M. Almonacid, M. Bussonnier, M.-H. Verlhac, N. Gov, P. Visco, F. van Wijland, and T. Betz, "Active mechanics reveal molecular-scale force kinetics in living oocytes," *Biophys. J.* **114**(7), 1667–1679 (2018).
- K. Luby-Phelps, "Cytoarchitecture and physical properties of cytoplasm: volume, viscosity, diffusion, intracellular surface area," *Int. Rev. Cytol.* **192**, 189–221 (1999).
- Y. Jun, S. K. Tripathy, B. R. Narayanareddy, M. K. Mattson-Hoss, and S. P. Gross, "Calibration of optical tweezers for in vivo force measurements: how do different approaches compare?" *Biophys. J.* **107**(6), 1474–1484 (2014).
- R. Vaipplu, V. Ramanujan, S. Bajpai, and B. Roy, "Measurement of viscoelastic properties of the cellular cytoplasm using optically trapped brownian probes," *J. Phys.: Condens. Matter* **32**(23), 235101 (2020).
- S. Hurst, B. E. Vos, M. Brandt, and T. Betz, "Intracellular softening and increased viscoelastic fluidity during division," *Nat. Phys.* **17**(11), 1270–1276 (2021).
- S. Roy, R. Vaipplu, M. Lokesh, G. Nalupurackal, P. Edwina, S. Bajpai, and B. Roy, "Comparison of translational and rotational modes towards passive rheology of the cytoplasm of mcf-7 cells using optical tweezers," *Front. Phys.* **10**, 1395 (2023).
- D. Robert, T.-H. Nguyen, F. Gallet, and C. Wilhelm, "In vivo determination of fluctuating forces during endosome trafficking using a combination of active and passive microrheology," *PLoS One* **5**(4), e10046 (2010).
- F. C. MacKintosh and C. F. Schmidt, "Active cellular materials," *Curr. Opin. Cell Biol.* **22**(1), 29–35 (2010).
- B. Stuhmann, M. S. e Silva, M. Depken, F. C. MacKintosh, and G. H. Koenderink, "Nonequilibrium fluctuations of a remodeling in vitro cytoskeleton," *Phys. Rev. E* **86**(2), 020901 (2012).
- S. Paul, B. Roy, and A. Banerjee, "Free and confined brownian motion in viscoelastic Stokes–Oldroyd B fluids," *J. Phys.: Condens. Matter* **30**, 345101 (2018).
- D. Martin, J. O'Byrne, M. E. Cates, E. Fodor, C. Nardini, J. Tailleur, and F. van Wijland, "Statistical mechanics of active orstein-uhlenbeck particles," *Phys. Rev. E* **103**(3), 032607 (2021).
- É. Fodor, R. L. Jack, and M. E. Cates, "Irreversibility and biased ensembles in active matter: Insights from stochastic thermodynamics," *Annu. Rev. Condens. Matter Phys.* **13**(1), 215–238 (2022).
- N. Koumakis, C. Maggi, and R. Di Leonardo, "Directed transport of active particles over asymmetric energy barriers," *Soft Matter* **10**(31), 5695–5701 (2014).
- C. Maggi, M. Paoluzzi, N. Pellicciotta, A. Lepore, L. Angelani, and R. Di Leonardo, "Generalized energy equipartition in harmonic oscillators driven by active baths," *Phys. Rev. Lett.* **113**(23), 238303 (2014).

34. M. Grimm, S. Jeney, and T. Franosch, "Brownian motion in a maxwell fluid," *Soft Matter* **7**(5), 2076–2084 (2011).
35. Y. L. Raikher and V. Rusakov, "Theory of brownian motion in a jeffreys fluid," *J. Exp. Theor. Phys.* **111**(5), 883–889 (2010).
36. Y. L. Raikher, V. V. Rusakov, and R. Perzynski, "Brownian motion in a viscoelastic medium modelled by a jeffreys fluid," *Soft Matter* **9**(45), 10857–10865 (2013).
37. E. J. Peterman, F. Gittes, and C. F. Schmidt, "Laser-induced heating in optical traps," *Biophys. J.* **84**(2), 1308–1316 (2003).
38. A. R. Bausch, W. Möller, and E. Sackmann, "Measurement of local viscoelasticity and forces in living cells by magnetic tweezers," *Biophys. J.* **76**(1), 573–579 (1999).
39. G. Guigas, C. Kalla, and M. Weiss, "Probing the nanoscale viscoelasticity of intracellular fluids in living cells," *Biophys. J.* **93**(1), 316–323 (2007).
40. T. G. Mason and D. A. Weitz, "Optical measurements of frequency-dependent linear viscoelastic moduli of complex fluids," *Phys. Rev. Lett.* **74**(7), 1250–1253 (1995).
41. A. W. Lau, B. D. Hoffman, A. Davies, J. C. Crocker, and T. C. Lubensky, "Microrheology, stress fluctuations, and active behavior of living cells," *Phys. Rev. Lett.* **91**(19), 198101 (2003).
42. P. Bursac, G. Lenormand, B. Fabry, M. Oliver, D. A. Weitz, V. Viasnoff, J. P. Butler, and J. J. Fredberg, "Cytoskeletal remodelling and slow dynamics in the living cell," *Nat. Mater.* **4**(7), 557–561 (2005).
43. D. Wirtz, "Particle-tracking microrheology of living cells: principles and applications," *Annu. Rev. Biophys.* **38**(1), 301–326 (2009).
44. H. Turlier, D. A. Fedosov, B. Audoly, T. Auth, N. S. Gov, C. Sykes, J.-F. Joanny, G. Gompfer, and T. Betz, "Equilibrium physics breakdown reveals the active nature of red blood cell flickering," *Nat. Phys.* **12**(5), 513–519 (2016).
45. P. Martin, A. Hudspeth, and F. Jülicher, "Comparison of a hair bundle's spontaneous oscillations with its response to mechanical stimulation reveals the underlying active process," *Proc. Natl. Acad. Sci.* **98**(25), 14380–14385 (2001).
46. R. Kubo, "The fluctuation-dissipation theorem," *Rep. Prog. Phys.* **29**(1), 255–284 (1966).
47. D. Mizuno, D. Head, F. MacKintosh, and C. Schmidt, "Active and passive microrheology in equilibrium and nonequilibrium systems," *Macromolecules* **41**(19), 7194–7202 (2008).
48. K. Umeda, K. Nishizawa, W. Nagao, S. Inokuchi, Y. Sugino, H. Ebata, and D. Mizuno, "Activity-dependent glassy cell mechanics ii, non-thermal fluctuations under metabolic activity," *arXiv arXiv:2302.13323* (2023).
49. M. Rief, R. S. Rock, A. D. Mehta, M. S. Mooseker, R. E. Cheney, and J. A. Spudich, "Myosin-v stepping kinetics: a molecular model for processivity," *Proc. Natl. Acad. Sci.* **97**(17), 9482–9486 (2000).
50. G. Cappello, P. Pierobon, C. Symonds, L. Busoni, J. Christof, M. Gebhardt, M. Rief, and J. Prost, "Myosin v stepping mechanism," *Proc. Natl. Acad. Sci.* **104**(39), 15328–15333 (2007).
51. A. D. Mehta, R. S. Rock, M. Rief, J. A. Spudich, M. S. Mooseker, and R. E. Cheney, "Myosin-v is a processive actin-based motor," *Nature* **400**(6744), 590–593 (1999).
52. C. Veigel, S. Schmitz, F. Wang, and J. R. Sellers, "Load-dependent kinetics of myosin-v can explain its high processivity," *Nat. Cell Biol.* **7**(9), 861–869 (2005).
53. M. Mittasch, P. Gross, and M. Nestler, *et al.*, "Non-invasive perturbations of intracellular flow reveal physical principles of cell organization," *Nat. Cell Biol.* **20**(3), 344–351 (2018).